

MHC class II function preserved by low-affinity peptide interactions preceding stable binding

Scheherazade Sadegh-Nasseri*[†],
Lawrence J. Stern[†], Don C. Wiley[‡]
& Ronald N. Germain*

* Lymphocyte Biology Section, Laboratory of Immunology, NIAID, National Institutes of Health, Bethesda, Maryland 20892, USA

[‡] Department of Biochemistry and Molecular Biology, and the Howard Hughes Medical Institute, Harvard University, Cambridge, Massachusetts 02138, USA

[†] Present addresses: Department of Immunology, American Red Cross Laboratories, 15601 Crabbs Branch Way, Rockville, MD 20855, USA (S.S.-N.); Department of Chemistry, Massachusetts Institute of Technology, Cambridge, MA 02139, USA (L.J.S.).

MAJOR histocompatibility complex class II molecules and their peptide ligands show unusual interaction kinetics, with slow association and dissociation rates that yield an apparent equilibrium constant of $\sim 10^{-6}$ – 10^{-8} M (refs 1–5). However, there is evidence for a specific, rapidly formed, short-lived complex⁶. The altered migration on SDS–polyacrylamide gel electrophoresis of class II molecules upon stable peptide binding^{7–9} has led to the hypothesis that the two kinetically distinguishable types of class II–peptide complexes correspond to different structures. In accord with this model, we demonstrate here that insect cell-derived HLA-DR1

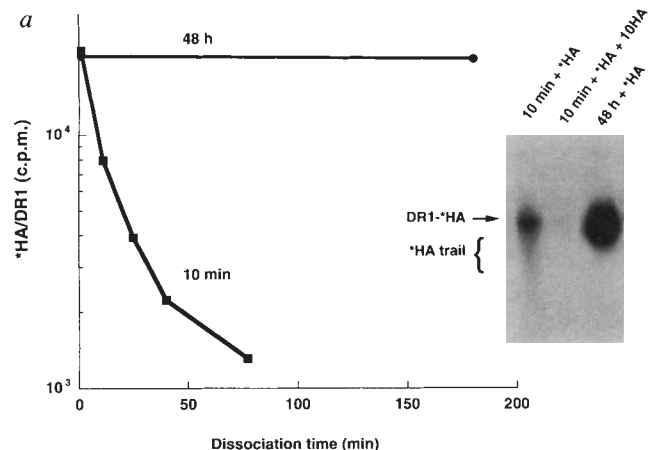
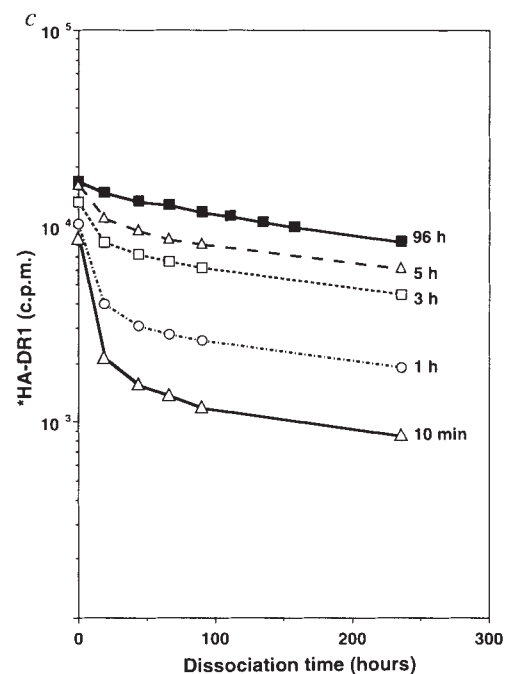
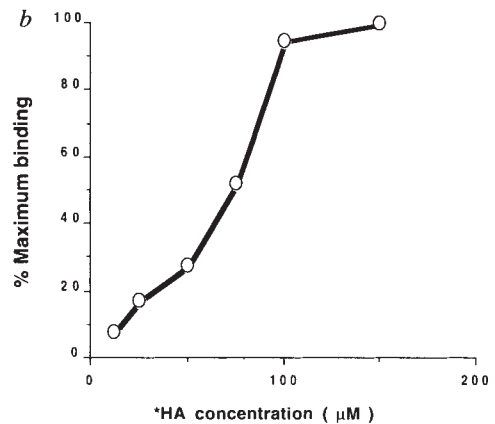


FIG. 1 Empty MHC class II molecules show both fast-on/fast-off and slow-on/slow-off interactions with a single peptide species. **a**, Peptide–DR1 complexes were formed by incubation of 0.3 μ M sDR1 with 100 μ M 125 I-labelled HA peptide (* HA) for 10 min or 48 h at 37 °C. After each incubation, peptide–DR1 complexes were separated from free peptide by spun column filtration and assayed by gamma counting. The kinetics of dissociation of complexes formed during 10 min of incubation were followed by subsequent sequential spun column separations. Inset (**a**), Peptide–DR1 complexes formed by incubation of sDR1 with 100 μ M 125 I-labelled HA peptide for 10 min or 48 h or with 125 I-labelled HA plus a 10-fold excess of unlabelled HA peptide for 10 min at 37 °C were analysed by native gel electrophoresis. **b**, Peptide–DR1 complexes formed by incubation of sDR1 with varying concentrations of 125 I-HA peptide for 10 min at 37 °C and analysed by spun column separation. **c**, Peptide–DR1 complexes were formed by incubation of sDR1 with 125 I-HA peptide for 10 min, 1, 3, 5 and 96 h at 37 °C. The kinetics of dissociation of complexes were measured as in **a**.

METHODS. Soluble DR1 was produced by L243 mAb-affinity purification of supernatant from Sf9 insect cells coinfecting with recombinant baculovirus encoding DR1 α and DR1 β chains truncated just before the transmembrane region⁹ or singly infected with recombinant baculovirus carrying both genes and a dual promoter (L.J.S., unpublished). Purified sDR1 was stored at 1–3 mg ml⁻¹ in phosphate-buffered saline (PBS),



pH 7.2, at 4 °C. Reverse-phase HPLC-purified HA 306–318 peptide (PKYVKQNTLKLAT) was labelled with 125 I using Iodobeads (Pierce) and separated from free iodine by passage through a 3-ml G-15 (Pharmacia) gel-filtration column. Fractions containing the labelled peptide were pooled and stored at 4 °C. HPLC analysis showed that the 125 I label coincided with the peptide peak. In most experiments the peptide pool was vacuum-concentrated to 2.5–3 mM ($6\text{--}7 \times 10^6$ c.p.m. per μ l). Peptide concentration was determined by tyrosine absorption or quantitative amino-acid analysis. Reaction mixtures contained sDR1 at 0.3 μ M and, unless otherwise indicated, peptide at 100 μ M in PBS in a total volume of 50 μ l. Spun columns (BioRad; 0.7 ml, containing BioGel P2) were blocked using 20% non-fat dry milk in PBS plus 0.02% Na₂S₂O₃, and used according to the manufacturer's recommendation. There was a linear correlation between the number of fast-forming complexes and the concentration of sDR1 used for incubation (S.S.N., unpublished observations), which indicates that labelled HA 306–318 binds to sDR1 and not to blocking proteins or other components of the assay system. For measurement of dissociation rates, peptide and sDR1 were mixed and incubated at 37 °C for the indicated times and passed through a spun column at room temperature. The excluded volume was collected, counted, and incubated for the first indicated dissociation time. It was then reapplied to a spun column and the excluded volume recovered and counted. This process was repeated to generate the data for the entire set of dissociation times. Native gel electrophoresis was performed using Mini-PROTEAN II Ready Gels from BioRad as described⁴. Dried gels were autoradiographed.

class II molecules show fast, almost stoichiometric occupancy with rapidly dissociating peptide while remaining sensitive to SDS-induced chain dissociation. The same DR1 molecules slowly and quantitatively form long-lived complexes resistant to SDS-induced denaturation. Surprisingly, low-affinity interaction with peptide protects class II from denaturation at physiological temperature, a finding that has implications for understanding the role of invariant chain in the intracellular behaviour of class II molecules.

Previous experiments in which fast-on/fast-off binding was observed used mouse class II molecules largely occupied with naturally processed peptides⁶. This resulted in measurements reflecting the properties of a small fraction of the class II. Here we examine the binding of a haemagglutinin (HA) peptide (residues 306–318) to soluble DR1 (sDR1) molecules produced by Sf9 insect cells. These secreted class II dimers are free of detectable peptide and bind offered ligand stoichiometrically⁹. Incubation of ¹²⁵I-labelled HA 306–318 with sDR1 for either 10 min or 48 h led to high levels of binding as measured by a rapid-separation technique (Fig. 1a). Fast-forming complexes could also be observed using native gels (Fig. 1a, inset). A relatively high concentration of peptide (100 μM) was required for rapid saturation binding (Fig. 1b), and the resulting complexes had a $t_{1/2\text{off}} \sim 10$ min (Fig. 1a), consistent with a low-affinity, fast-on/fast-off interaction. In contrast, sDR1–HA complexes generated at longer incubation times showed an increasing proportion of long-lived forms, whose $t_{1/2\text{off}}$ was ~ 140 h at 37 °C (Fig. 1c). The complexes generated upon prolonged incubation showed

occupancy approaching 100%. Owing to their rapid dissociation rate, small changes in separation time led to greater variability in the measured number of rapidly forming complexes, ranging over 50–90% of maximum binding. These data are consistent with the same DR1 molecule binding peptide in either of two states.

Rapid peptide binding is specific. sDR1 showed rapid binding to HA 306–318 but not to a moth cytochrome *c* peptide (residues 88–103), whereas this latter peptide but not HA showed fast-on/fast-off binding to purified $E\alpha^k E\beta^k$ (Fig. 2a). This also demonstrates that fast-on/fast-off binding is not unique to the sDR1–HA combination, and occurs with class II molecules produced by normal B cells coexpressing invariant chain. Cold HA 306–318 competes for labelled peptide binding in direct proportion to its concentration (Fig. 2b) and incubation of sDR1 with mixtures of labelled and unlabelled HA having a constant total peptide concentration give a linear binding relationship with a slope of 1 with respect to the concentration of labelled peptide for both types of complexes (Fig. 2c). These latter data argue strongly against the possibility that peptide–DR1 complexes with different off rates arise from heterogeneous iodination of HA 306–318 at the tyrosine involved in high-affinity binding^{4,10,11}.

Stable binding of peptide to class II heterodimers induces a change in the biochemical properties of the major histocompatibility complex (MHC) molecules^{8,9,12,13}. Increased resistance to subunit dissociation during SDS–PAGE is a convenient assay

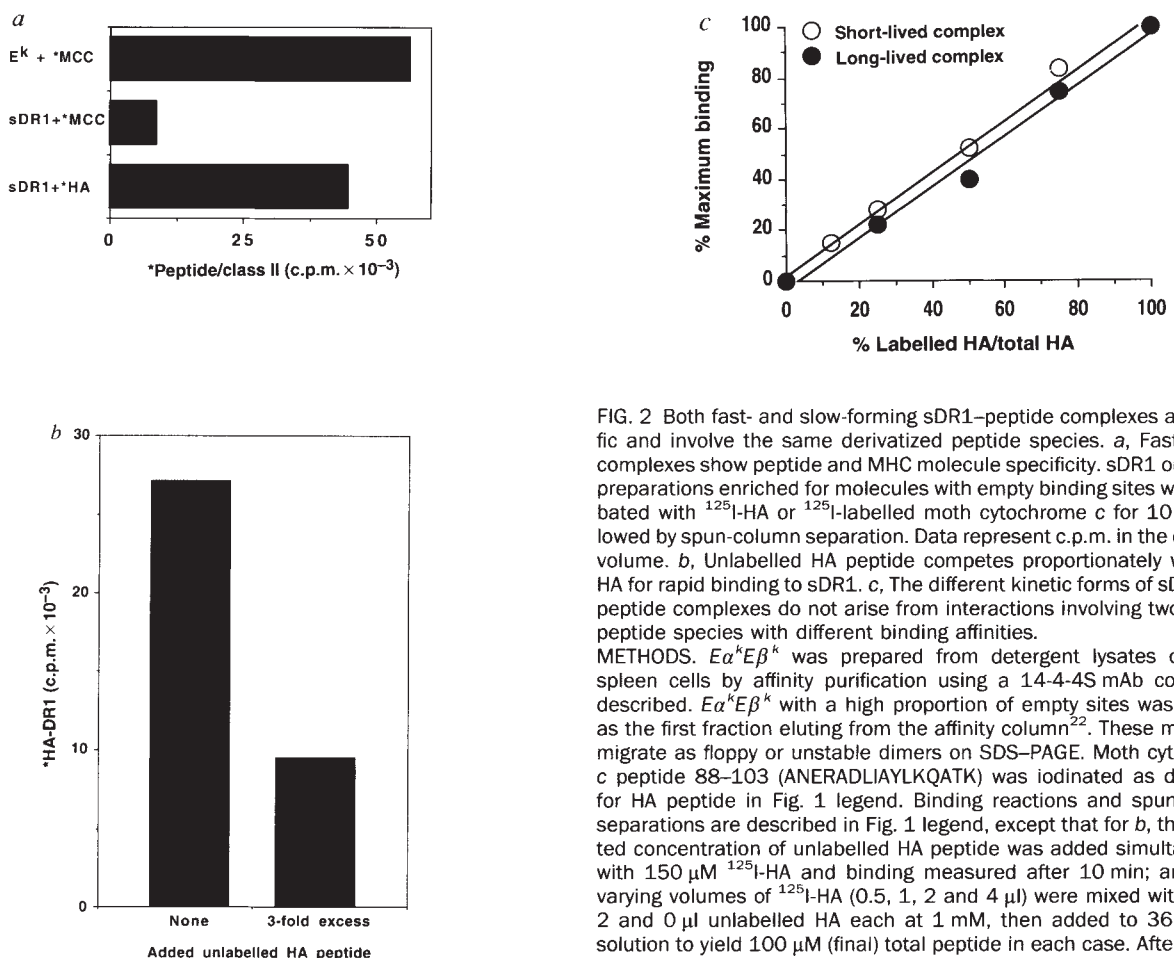
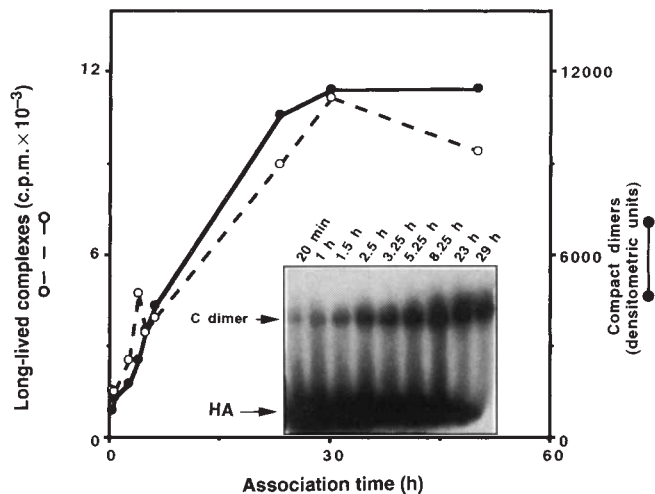


FIG. 2 Both fast- and slow-forming sDR1–peptide complexes are specific and involve the same derivatized peptide species. **a**, Fast-forming complexes show peptide and MHC molecule specificity. sDR1 or $E\alpha^k E\beta^k$ preparations enriched for molecules with empty binding sites were incubated with ¹²⁵I-HA or ¹²⁵I-labelled moth cytochrome *c* for 10 min, followed by spun-column separation. Data represent c.p.m. in the excluded volume. **b**, Unlabelled HA peptide competes proportionately with ¹²⁵I-HA for rapid binding to sDR1. **c**, The different kinetic forms of sDR1/HA-peptide complexes do not arise from interactions involving two distinct peptide species with different binding affinities.

METHODS. $E\alpha^k E\beta^k$ was prepared from detergent lysates of CBA/J spleen cells by affinity purification using a 14-4-4S mAb column as described. $E\alpha^k E\beta^k$ with a high proportion of empty sites was isolated as the first fraction eluting from the affinity column²². These molecules migrate as floppy or unstable dimers on SDS–PAGE. Moth cytochrome *c* peptide 88–103 (ANERADLIYLKQATK) was iodinated as described for HA peptide in Fig. 1 legend. Binding reactions and spun column separations are described in Fig. 1 legend, except that for **b**, the indicated concentration of unlabelled HA peptide was added simultaneously with 150 μM ¹²⁵I-HA and binding measured after 10 min; and for **c**, varying volumes of ¹²⁵I-HA (0.5, 1, 2 and 4 μl) were mixed with 3.5, 3, 2 and 0 μl unlabelled HA each at 1 mM, then added to 36 μl sDR1 solution to yield 100 μM (final) total peptide in each case. After incubation for 10 min or 48 h at 37 °C, incubation mixtures were subjected to spun-column separation, and the excluded volume was counted. The figure displays the relationship between the concentration of labelled peptide and extent of complex formation.



for this change, although this pattern of electrophoretic behaviour is not seen with all long-lived class II-peptide combinations^{12,14,15}. Brief incubation with unlabelled HA did not induce any detectable change in the migration pattern of sDR1 in SDS-PAGE, as both empty and rapidly loaded DR1 migrated as dissociated chains under these conditions (data not shown). A kinetic analysis of stable (compact) dimer and long-lived complex formation is shown in Fig. 3. The total labelled peptide signal from HA-sDR1 complexes (short lived plus long lived) at different incubation times was relatively constant. Formation of compact dimers (Fig. 3, solid circles and inset) and long-lived peptide-sDR1 complexes (Fig. 3, open circles) occurred at the same rate, with a $t_{1/2}$ on ~ 7 h at 37 °C. As more compact dimers formed, fewer short-lived complexes were detected, as indicated by a smaller free peptide signal at the dye front (Fig. 3, inset). Thus, most or all sDR1 molecules have binding sites able to form complexes with peptide rapidly, but generation of long-lived complexes occurs in parallel with an infrequent structural change that takes place in the population of peptide-interacting sDR1 molecules with a $t_{1/2}$ of 6–7 h.

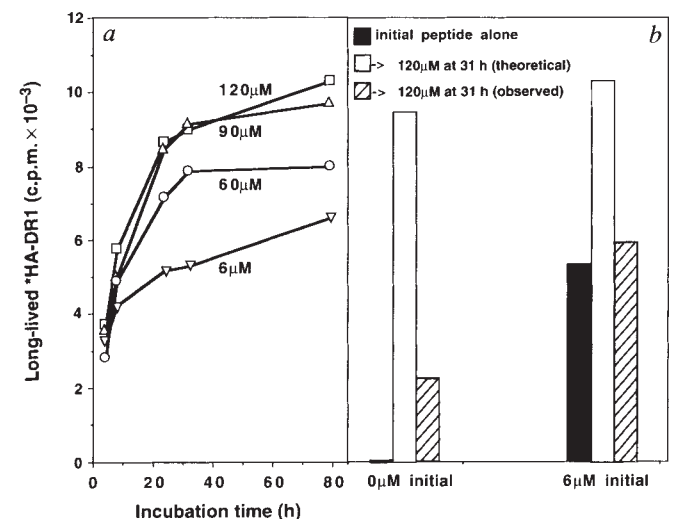
While investigating stable complex formation at varying peptide concentrations, we noted that each concentration led to different plateau binding, despite the use of at least a 20-fold molar excess of peptide over sDR1 (Fig. 4a). Furthermore, once long-lived complex formation approached a plateau at a sub-saturating peptide concentration, addition of a saturating concentration of ligand did not yield the predicted number of additional long-lived complexes (Fig. 4b), suggesting that most sDR1 molecules that had not formed stable complexes by this

FIG. 4 Peptide concentration-dependent survival of sDR1 molecules at 37 °C. **a**, sDR1 was incubated at 37 °C with ¹²⁵I-HA peptide (0, 6, 60, 90 and 120 μ M) for the times indicated. Long-lived peptide-sDR1 complexes were quantified for each incubation time by two sequential spun-column separations (Fig. 3 legend). **b**, Samples incubated for 31 h with 6 or 0 μ M peptide at 37 °C were each split into two tubes and additional peptide was added to one sample of each group to raise the final concentration of peptide to 120 μ M. These samples were further incubated at 37 °C for 48 h and then analysed by sequential spun-column separation for long-lived complex formation. **METHODS**. A cocktail of protease inhibitors was included in the sDR1 preparation⁹ to inhibit proteolysis, and no significant class II α - or β -chain degradation was observed under these incubation conditions as assayed by SDS-PAGE or native gel electrophoresis.

time had become functionally inactive or denatured. The plateau of stable complex formation roughly correlated with the levels of fast-dissociating complexes generated at each peptide concentration (Fig. 1b), implying that formation of rapidly dissociating complexes preserves class II from binding site inactivation at physiological temperature. These experiments provide strong evidence for two distinct kinetic modes of interaction involving a single peptide-MHC class II pair. The demonstration of both binding states using distinct peptides and different class II molecules from humans and mice suggests that these two binding states may be a common, though not always readily detectable, characteristic of class II-peptide reactions. Our results are also important in that they demonstrate the near-stoichiometric occupancy of the same population of class II molecules with either rapidly or slowly dissociating peptide. This rules out the possibility that fast-on/fast-off binding reflects the behaviour of a subset of class II molecules structurally incapable of stable peptide acquisition. Experiments with living cells suggest that fast-on/fast-off binding can be physiologically relevant¹⁶. Our data also make clear that the slow formation of long-lived class II-peptide complexes can be only partially accounted for by the gradual generation of new binding sites from class II molecules preoccupied with naturally processed peptides¹⁷, as sDR1 molecules whose binding sites are uniformly accessible to peptide in as little as 10 min still show a forward $t_{1/2}$ of 5–7 h for formation of stable complexes at neutral pH. Formation of long-lived complexes occurs at the same rate as a change in class II biochemical behaviour, revealed for the

FIG. 3 The two different kinetic forms of peptide-sDR1 complexes correlate with distinct structural states of the sDR1 molecules; quantitative and kinetic correlation between the formation of slowly dissociating peptide-sDR1 complexes and the formation of compact, SDS-resistant sDR1 dimers. Mixtures of labelled HA peptide and sDR1 were incubated for the indicated times, then separated on two sequential spun columns to measure slowly dissociating complexes (open circles), or subjected to SDS-PAGE (inset) and autoradiography to determine the extent of compact SDS-resistant dimer (C dimer) formation (filled circles). **METHODS**. Mixtures of sDR1 and labelled HA peptide were incubated for the times shown. Part of each mixture was then subjected to SDS-PAGE followed by autoradiography⁸. The compact dimer signal seen in the inset was determined by densitometry and plotted as a function of time. Stable complexes were analysed using the other portion of each mixture by two sequential spun column separations, allowing 3 hours between the first and second separations to permit dissociation of rapidly forming complexes. Similar levels of total binding (fast-off + slow-off) were seen at early and late times of incubation (at 1 h, 14,553 c.p.m.; at 48 h, 13,638 c.p.m.)

FIG. 4 **a**, Kinetic analysis of peptide-sDR1 complexes. The graph shows Long-lived *HA-DR1 (c.p.m. x 10⁻³) on the y-axis (0 to 12) versus Incubation time (h) on the x-axis (0 to 80). Five curves are shown for peptide concentrations: 120 μ M (filled squares), 90 μ M (open triangles), 60 μ M (open circles), 6 μ M (open inverted triangles), and 0 μ M (open squares). **b**, Bar graph showing Long-lived *HA-DR1 (c.p.m. x 10⁻³) for two initial peptide concentrations: 0 μ M and 6 μ M. For each, two bars are shown: 'initial peptide alone' (solid black) and '120 μ M at 31 h (theoretical)' (open white). For 6 μ M initial, a third bar shows '120 μ M at 31 h (observed)' (hatched).



sDR1-HA combination as enhanced stability during SDS-PAGE. Thus, in accord with the kinetic-intermediate model⁶, the slow event in peptide binding correlates with a change in class II dimer structure. The rare nature of this structural change among rapidly occupied class II molecules might be due either to an intrinsic energetic barrier for conversion of class II to this higher-affinity state, or to the low frequency with which an interacting peptide is optimally oriented in the binding groove. The latter possibility is consistent with the chemistry of HA peptide interaction with DR1 molecules that involves conserved hydrogen bonds between class II and the main-chain atoms of the peptide, as well as many peptide side-chain/DR1 interactions¹⁰. These properties could permit class II to interact weakly with a peptide whose side-chain anchors do not all sit properly in pockets within the binding groove, and suggest that stable binding occurs when the side chains and pockets are aligned properly.

An intriguing finding is the ability of low-affinity peptide occupancy to preserve class II from the inactivation at physiological temperature. We and others have reported that invariant chain is important in stabilizing the association of class II α - and β -subunits within living cells without yielding the SDS-resistant phenotype¹⁸⁻²⁰. The ability of low-affinity peptide binding to preserve class II heterodimers without promoting their resistance to SDS denaturation raises the possibility that a similar quality of binding site occupancy by a segment of intact invariant chain helps maintain the function of class II

molecules until they arrive at an endosomal site appropriate for antigen capture^{21,22}. □

Received 5 April; accepted 15 July 1994.

- Babbitt, B. P., Allen, P. M., Matsueda, G., Haber, E. & Unanue, E. R. *Nature* **317**, 359-361 (1985).
- Buus, S., Sette, A., Colon, S. M., Jenis, D. M. & Grey, H. M. *Cell* **47**, 1071-1077 (1986).
- Roche, P. A. & Cresswell, P. *J. Immunol.* **144**, 1849-1856 (1990).
- Jardetzky, T. S. et al. *EMBO J.* **9**, 1797-1803 (1990).
- Roof, R. W., Leuschner, I. F. & Unanue, E. R. *Proc. natn. Acad. Sci. U.S.A.* **87**, 1735-1739 (1990).
- Sadegh-Nasseri, S. & McConnell, H. M. *Nature* **337**, 274-276 (1989).
- Wettstein, D. A., Boniface, J. J., Reay, P. A., Schild, H. & Davis, M. M. *J. exp. Med.* **174**, 219-228 (1991).
- Sadegh-Nasseri, S. & Germain, R. N. *Nature* **353**, 167-170 (1991).
- Stern, L. J. & Wiley, D. C. *Cell* **68**, 465-477 (1992).
- Stern, L. J., Brown, J. H., Jardetzky, T. S. & Wiley, D. C. *Nature* **368**, 215-221 (1994).
- Hammer, J. et al. *Cell* **74**, 197-203 (1993).
- Germain, R. N. & Rinker, A. G. Jr *Nature* **363**, 725-728 (1993).
- Kozono, H., White, J., Clements, J., Marrack, P. & Kappler, J. *Nature* **369**, 151-154 (1994).
- Lanzavecchia, A., Reid, P. A. & Watts, C. *Nature* **357**, 249-252 (1992).
- Nelson, C. A., Petzold, S. J. & Unanue, E. R. *Proc. natn. Acad. Sci. U.S.A.* **90**, 1227-1231 (1993).
- Fairchild, P. J., Wildgoose, R., Atherton, E., Webb, S. & Wraith, D. C. *Int. Immun.* **5**, 1151-1158 (1993).
- Tampe, R. & McConnell, H. M. *Proc. natn. Acad. Sci. U.S.A.* **88**, 4661-4665 (1991).
- Viville, S. et al. *Cell* **72**, 635-648 (1993).
- Bikoff, E. K. et al. *J. exp. Med.* **177**, 1699-1712 (1993).
- Bonnerot, C. et al. *EMBO J.* **13**, 934-944 (1994).
- Romagnoli, P. & Germain, R. N. *J. exp. Med.* (in the press).
- Sadegh-Nasseri, S. in *Antigen Processing and Presentation* (eds Humphreys, R. E. & Pierce, S. K.) 170-187 (Academic, San Diego, 1994).

ACKNOWLEDGEMENTS. S.S.N. was supported in part by Oravax, Inc. L.J.S. acknowledges a fellowship from the Daymon Runyon-Walter Winchell Cancer Institute; D.C.W. is an investigator with the Howard Hughes Medical Institute. We thank D. Margulies for discussion and for reviewing the manuscript.

Cytolytic T-cell cytotoxicity is mediated through perforin and Fas lytic pathways

Bente Lowin, Michael Hahne, Chantal Mattmann & Jürg Tschopp*

Institute of Biochemistry, University of Lausanne, CH-1066 Epalinges, Switzerland

THE recent generation of perforin knock-out mice^{1,2} has demonstrated a crucial role for the pore-forming perforin in cytolytic T-lymphocyte (CTL)-mediated cytotoxicity. Perforin-deficient mice failed to clear lymphocytic choriomeningitis virus *in vivo*, yet substantial killing activity still remained in perforin-free CTLs *in vitro*, indicating the presence of (a) further lytic pathway(s). Fas is an apoptosis-signalling receptor molecule on the surface of a number of different cells. Here we report that both perforin-deficient and Fas-ligand-deficient CTLs show impaired lytic activity on all target cells tested. The killing activity was completely abolished when both pathways were inactivated by using target cells from Fas-receptor-deficient *lpr* mice and perforin-free CTL effector cells. Fas-ligand-based killing activity was triggered upon T-cell receptor occupancy and was directed to the cognate target cell. Thus, two complementary, specific cytotoxic mechanisms are functional in CTLs, one based on the secretion of lytic proteins and one which depends on cell-surface ligand-receptor interaction.

The analysis of perforin-deficient mice has revealed the important role of perforin in CTL-mediated cytotoxicity^{1,2}. While Kägi *et al.* concluded from their results that perforin accounts for 100% of the lytic activity against most target cells¹, we measured substantial lysis of all haematopoietic target cells, when apoptosis rather than plasma membrane damage was taken as an indicator for cell death². Moreover, using adherent instead of

trypsin-detached cells, one-third of the killing activity remained² with fibroblasts as target cells. To corroborate the presence of alternative perforin-independent killing pathways, major histocompatibility complex (MHC) alloantigen-specific cytotoxicity of C57BL/6 (H-2^b) anti-MRL (H-2^k) cultures was assayed on additional target cells, including mouse primary embryonic fibroblasts, the L929 fibroblast cell line and concanavalin A (conA)-stimulated lymphocytes. Although cytotoxicity was impaired in the absence of perforin, all target cells were considerably lysed (Fig. 1a-c). The residual lytic activity persisted in perforin-deficient CTLs, when lysis was redirected to nonspecific targets via T-cell-receptor-specific antibodies (Fig. 1d).

The cell-surface receptor Fas can transduce signals which lead to apoptotic cell death^{3,4}. The Fas-based death pathway plays an important regulatory role *in vivo*. *lpr* mice, devoid of functional Fas receptor (FasR)⁵, as well as *gld* mice, lacking the active Fas ligand (FasL)^{6,7}, suffer from similar auto-immune pathologies, including the accumulation of large numbers of lymphocytes in spleen and lymph nodes. Fas also contributes to nonspecific CTL cytotoxicity observed after polyclonal activation of lymphocytes^{8,9}.

To evaluate the contribution of Fas in specific CTL cytotoxicity, mixed lymphocyte cultures of *gld*-derived spleen cells (FasL⁻) were generated. Fibroblasts as well as conA-stimulated lymphoblasts were lysed by FasL-deficient lymphocytes, albeit with reduced activity compared to wild-type CTLs (Fig. 1a-d). The cytolytic activity was comparable to that detected with perforin-deficient CTLs. About 10-30% of killing activity was left in each case. Experiments were now devised whereby both pathways were functionally inactive (Fig. 2). Target cells were derived from the C3H/*lpr* mice (FasR⁻). Normal CTLs (perforin⁺/FasL⁺) as well as *gld*-derived CTLs (FasL⁻) still showed lytic activity (presumably perforin-based). In contrast, perforin-deficient CTLs were completely inactive against FasR-lacking primary fibroblasts or lymphocyte targets. Thus, Fas- and perforin-dependent pathways are responsible for all detectable killing activity in these experimental systems.

Target-cell recognition and killing by CTLs is highly specific, sparing bystander cells, that is, non-cognate targets mixed

* To whom correspondence should be addressed.